Rate of Incision of *N*-Acetyl-2-aminofluorene and *N*-2-Aminofluorene Adducts by UvrABC Nuclease Is Adduct- and Sequence-Specific: Comparison of the Rates of UvrABC Nuclease Incision and Protein−DNA Complex Formation†

Olga Mekhovich,‡ Moon-shong Tang,§ and Louis J. Romano*,‡

Department of Chemistry, Wayne State University, Detroit, Michigan 48202, and University of Texas M. D. Anderson Cancer Center, Science Park−Research Division, Smithville, Texas 78957

Received June 26, 1997; Revised Manuscript Received October 2, 1997⊗

ABSTRACT: The UvrABC nuclease, the nucleotide excision repair complex from *Escherichia coli*, is able to incise a variety of types of DNA damage and the repair efficiency of this enzyme complex appears to be influenced by the structure of the damage and the sequence context within which the damage is positioned. In order to better establish these relationships, we have constructed two DNA sequences each containing a site-specifically positioned *N*-2-aminofluorene (AF) or *N*-acetyl-2-aminofluorene (AAF) adduct and have determined both the kinetics of UvrABC nuclease incision and the kinetics of UvrABC nuclease−substrate complex formation. It is well established that these two adducts induce very different structures in the DNA and that these structures also depend on the sequence context. We have found that the rate of incision of both AAF− and AF−DNA adducts is significantly faster when they are positioned in the mutation hotspot *Nar*I sequence (5-GGCG*CC-3′) than when located in a normal or non-*Nar*I sequence (5′-GATG*ATA-3′) and that the rate of incision for AAF−DNA adducts is faster that for AF adducts in both sequences. Most siginificantly, we find that the rate of UvrB and UvrBC−substrate complex formation correlates with the rate of UvrABC nuclease incision.

One of the most remarkable and enigmatic features of the UvrABC nuclease from *Escherichia coli* is its versatility in the recognition and repair of a large variety of DNA lesions. These DNA lesions include AP sites, lesions of cisplatin (Alazard et al., 1982), psoralen (Sancar & Rupp, 1983), *N*-acetyl-2-aminofluorene (Tang et al., 1982; Pierce et al., 1989), ultraviolet light (Sancar & Rupp, 1983) anthramycin (Pierce et al., 1989), and even complexes of noncovalent DNA binding chemicals (Lambert et al., 1989; Selby & Sancar, 1991). Due to this diversity, the physical and chemical characteristics of DNA helix distortion sufficient for recognition by UvrABC enzyme are not completely understood. However, it appears that the efficiency of DNA repair is influenced not only by the chemical structure of the lesion but also by the helix topology and the DNA sequence in the proximity of the lesion (Jones & Yeung, 1988; Seeberg & Fuchs, 1990; Ramaswamy & Yeung, 1994).

It has been proposed that the high specificity of the DNA repair by the UvrABC nuclease is achieved through a "selectivity cascade" (Lin & Sancar, 1992). Initially, the UvrA protein dimerizes in solution and then assembles into a $UvrA_2B$ complex on the DNA. The affinity of UvrA protein for the DNA lesion guides this complex to the damaged site after which the UvrA subunit dissociates (Orren & Sancar, 1989). Because the degree of selectivity of the UvrA protein for DNA lesions over nondamaged DNA is modest, it has been referred to as the "proximal damage recognition subunit" (Hsu et al., 1995). Following dissociation of the UvrA subunit, the UvrB protein forms a stable protein−DNA complex that is locally denatured by 5−6 bp around the lesion and bent by 130° (Sancar & Tang, 1993). The UvrB protein binds very strongly to damaged DNA, suggesting that this subunit determines the efficiency of removal of a lesion from DNA. Therefore, it has been referred to as the "ultimate damage recognition subunit". The UvrB protein apparently has a hydrophobic pocket where the modified DNA bases fit. The size of the lesion and its degree of hydrophobicity are among the characteristics that contribute to the ability of a lesion to function as a substrate for the UvrB protein (Hsu et al., 1995).

Upon the binding of the UvrC subunit to the UvrB protein−DNA complex, the DNA strand is apparently cleaved on the 3′ side of the adduct by the UvrB protein and on the 5′ side by the UvrC protein (Sancar, 1996). Thus the formation of the UvrB protein−DNA complex is not sufficient for the 3′ cleavage incisions, and it has been suggested that a UvrC protein-induced conformational change must occur in the UvrB protein−DNA complex before the incision is made (Hsu et al., 1994; Moolenaar et al., 1995). Support for this idea includes the fact that for cisplatin lesions the binding of the UvrC protein to the UvrB protein−DNA complex is fast relative to incision, suggesting

† This investigation was supported by Public Health Service Grants CA40605 (L.J.R.) and ES03124 and ES08389 (M.s.T.) awarded by the Department of Health and Human Services.

* To whom correspondence should be addressed. Tel. 313-577-2584; Fax 313-577-8822; E-mail ljr@chem.wayne.edu.

‡ Wayne State University.

§ University of Texas M. D. Anderson Cancer Center.

⊗ Abstract published in *Advance ACS Abstracts,* December 15, 1997.

S0006-2960(97)01544-4 CCC: $15.00
Published on Web 01/13/1998

this conformational change may have to occur before cleavage can take place (Snowden & Van Houten, 1991). Although the 3′ and 5′ incisions are thought to be nearly concerted, the 3′ incision is apparently made first, followed rapidly by the 5′ cleavage (Lin et al., 1992).

Aromatic amines are an important class of chemical carcinogens, and *N*-acetyl-2-aminofluorene (AAF)[1] is a well-studied example of this class. Animal exposure results in the formation of two major adducts, *N*-(2′-deoxyguanosin-8-yl)-2-(acetylamino)fluorene (dG-C8-AAF) and *N*-(2′-deoxyguanosin-8-yl)-2-aminofluorene (dG-C8-AF) (King, 1985), and these two adducts are readily recognized by the UvrABC nuclease (Pierce et al., 1989). Interestingly, these adducts show very different biological properties in terms of mutagenicity in bacteria: the dG-C8-AF adduct produces mostly base substitution mutations, whereas the dG-C8-AAF adduct is more prone to induce frameshift mutations (Bichara & Fuchs; 1985; Koffel-Schwartz et al., 1984). In addition, dG-C8-AAF adducts show preferential mutagenesis in certain sequences. One of these hotspots is the recognition sequence for the restriction enzyme *Nar*I (5′-GGCGCC-3′) (Koffel-Schwartz et al., 1984), where GC deletions were observed to occur at a high frequency. Subsequently, it was shown that the mutation frequency and specificity varied with respect to the position of the AAF adduct within this sequence and that the GC dinucleotide deletion occurred only when the adduct was bound to the G_3 position (Burnouf et al., 1989). Placement of an AF adduct at this same position did not result in this deletion (Tebbs & Romano, 1994), suggesting that this adduct adopts a very different structure in this sequence.

Most spectral and theoretical studies suggest that the AF structure produces less distortion in the DNA helix than the AAF adduct (Singer & Grunberger, 1984; Hingerty & Broyde, 1986; van Houte et al., 1987, 1988; Belguise-Vallandier & Fuchs, 1991). Multidimensional NMR studies reveal that the guanine bearing the AAF adduct has rotated from the *anti* to the *syn* conformation so that the fluorene ring is inserted into the helix (base displacement model) (O'Handley et al., 1993). Similar studies on AF-modified DNA suggests that these adducts can adopt interchangeable conformations: a major one in which the fluorene remains outside the helix (outside binding model) and minor conformers where the fluorene is stacked within the helix (Norman et al., 1989; Eckel & Krugh, 1994; Cho et al., 1994). Chemical modification studies (Belguise-Valladier & Fuchs, 1991) and circular dichroism experiments (Koehl et al., 1989) suggest that AAF modification at the G_3 position of the *Nar*I sequence leads to a major alteration of the helix structure. Interestingly, chemical probing of AF-modified DNA containing the *Nar*I site (Belguise-Valladier & Fuchs, 1995) revealed that modification of G_3 also resulted in extensive reaction with chemical agents, again suggestive of a distortion in the helix.

In the present study, we have determined the rates of incision by the UvrABC nuclease for AAF and AF adducts positioned at G_3 of the *Nar*I sequence or in a non-hotspot sequence 5′- ATG$^{(x)}$ATA -3′ and simultaneously measured the rate of preincision and incision complex formation. We find that the rate of cleavage is sequence- and adduct-dependent and that the rate of preincision UvrBC−DNA complex formation correlates with the rate of incision.

EXPERIMENTAL PROCEDURES

Materials

Enzymes. UvrA, UvrB, and UvrC proteins were purified as described previously (Tang, 1996).

T4 polynucleotide kinase was purchased from USB, and T4 DNA ligase was obtained from New England Biolabs. The protein molecular weight markers were purchased from Sigma (cross-linked phosphorylase *b*, 97 400 Da, monomer through hexamer, and cross-linked albumin, 66 000 Da, monomer through tetramer).

Oligonucleotides. All synthetic oligonucleotides were obtained from Midland Certified Inc. Site-specifically modified 12-mers, d[GTGGCG$^{(C8-AAF)}$CCAAGT] and d[GTGATG$^{(C8-AAF)}$ATAAGT] were obtained and purified as described by Zhou (Zhou & Romano, 1993). AF-containing 12-mers were obtained by deacetylation of AAF-12-mers as described by Shibutani et al. (1991).

Reagents and Buffers. [γ-^{32}P]ATP was from ICN Biomedicals. Glutaraldehyde [50% (v/v) water solution] was purchased from Aldrich. All other reagents were obtained from various chemical houses and were the highest quality available.

Methods

Construction of Double-Stranded Oligonucleotides with Single AAF or AF Adducts. All synthetic oligonucleotides were first purified by polyacrylamide gel electrophoresis. Site-specifically AAF or AF modified 12-mers were labeled at the 5′ end with [γ-^{32}P]ATP (7000 Ci/mmol) and T4 polynucleotide kinase. The oligonucleotide (25-mer) to be linked to the 3′ end of the modified 12-mer (see Figure 1) was phosphorylated with nonradiolabeled ATP and T4 polynucleotide kinase at its 5′-end. These two phosphorylated oligonucleotides were mixed with the 25-mer that was to be ligated to the 5′ side of the modified 12-mer and a complementary 54-mer. Equal amounts (50 pmol) of the oligonucleotides were used except that the modified 12-mer was present in a 3-fold excess (150 pmol). The reaction was carried out in a 500 μL volume. After incubation at 65 °C for 15 min and slow cooling, the oligonucleotides were ligated with 1200 units of T4 DNA ligase at 16 °C for 2 h using the protocol recommended by the manufacturer (New England Biolabs). The ligated 62-mer containing the adduct and the complementary 54-mer were denatured and fractionated on an 8% polyacrylamide gel in the presence of 7 M urea. The modified 62-mer was then recovered from the gel and purified by ethanol precipitation. The purity of the product was verified using a 15% denaturing gel electrophoresis. This oligonucleotide was reannealed to the unlabeled complementary 62-mer and purified on a 15% nondenaturing polyacrylamide gel. The resulting construct was eluted from the gel and repurified by ethanol precipitation.

Gradient SDS−PAGE Analysis To Determine the Molecular Mass of the Cross-Linked UvrABC Protein−DNA

[1] Abbreviations: AAF; *N*-acetyl-2-aminofluorene; AF; *N*-2-aminofluorene; dG-C8-AAF, *N*-(2′-deoxyguanosin-8-yl)-2-(acetylamino)-fluorene; dG-C8-AF, *N*-(2′-deoxyguanosin-8-yl)-2-aminofluorene; PAGE; polyacrylamide gel electrophoresis; TBE, 90 mM Tris−borate and 2 mM EDTA, pH 8.3.

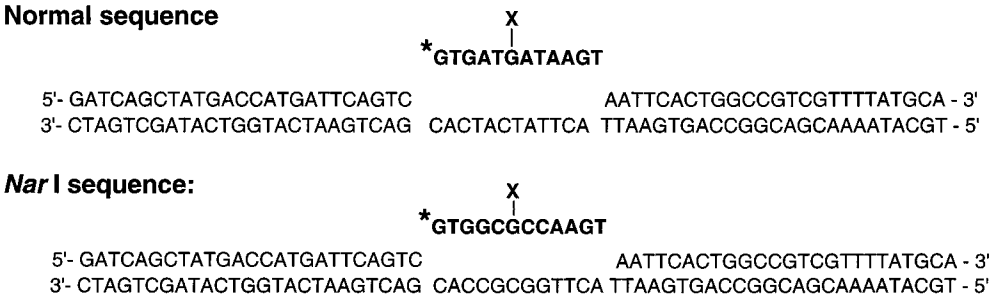

FIGURE 1: Schematic representation for the construction of site-specifically modified oligonucleotides. The AAF- and AF-modified oligonucleotides were constructed by the ligation of two 25-mers to a central ^{32}P-labeled, modified 12-mer, each of which was annealed to a complementary 62-mer. X = AAF or AF; an asterisk indicates ^{32}P.

Complexes. DNA binding reactions of the UvrABC nuclease were carried out in 100 μL of the buffer, containing 5 mM Tris-HCl, pH 7.5, 10 μM EDTA, 0.1 mM DTT, 1 mM $MgCl_2$, 0.1 mM ATP, and 0.1 M KCl. The reaction mixture contained DNA at the concentration indicated (0.5−1 nM) and 50 nM UvrABC proteins. The mixture was incubated at 37 °C for 15 min, treated for 1 min with freshly diluted glutaraldehyde 0.025% (v/v), and irradiated with UV light (305 nm) for 15 min at an intensity of 2 mW/cm^2. To precipitate cross-linked proteins, a 0.5× volume of 20% trichloroacetic acid (TCA) was added into each reaction mixture. These samples were stored on ice for 15 min prior to centrifugation at 15 000 rpm and 4 °C for 15 min. The pellets were washed twice with ice-cold acetone and dried in air; after that, each of them was redissolved in 20 μL of loading buffer containing 0.1 M $NaPO_4$ (pH 7.0), 1% SDS, 36% (w/v) urea, 100 mM 2-mercaptoethanol, and 0.1% bromophenol blue. The samples were loaded onto an SDS gradient (4−8%) polyacrylamide gel cast in the Weber−Osborn buffer system (Weber & Osborn, 1969). Electrophoresis was carried out at 50 V. The molecular weight markers were visualized by staining with Coomassie blue, and the amount of radioactivity was determined by scanning the gel with a Molecular Dynamics PhosphorImager.

Incision Assay and DNA−Protein Cross-Linking. The UvrABC nuclease reaction was the same as described above. To determine the kinetics of Uvr protein binding and incision, aliquots (100 μL) were taken at time points 0, 2, 5, 10, 20, and 30 min. A portion of each aliquot (10 μL) was mixed with formamide denaturing loading buffer and immediately denatured by heating to 95 °C and cooling on ice. To the remaining portion (90 μL) of each aliquot was added 10 μL of a diluted glutaraldehyde solution to a final concentration of 0.025%. The mixtures were incubated for 1 min on ice and then subjected to the UV cross-linking as described above. Then a portion of each sample (10 μL) was taken again and mixed with the formamide denaturing loading buffer and denatured. All denatured reaction mixtures (before and after cross-linking) were fractionated on a 15% denaturing gel cast in Tris−borate−EDTA (TBE) buffer. The remaining samples (90 μL each) were precipitated by trichloroacetic acid, and the pellets were redissolved in $NaPO_4$ loading buffer and loaded on an SDS−polyacrylamide gradient (4−8%) gel cast in the Weber−Osborn buffer system (Weber & Osborn, 1969) as described above. The percentage of incised product and protein−DNA complex formed was calculated with respect to total amount of radioactivity in each lane.

RESULTS

Incision of DNA Containing AAF and AF Adducts Is Dependent on the Sequence Context. Two sequences were used for these analyses. The first was a sequence that is not mutation-prone and is not predicted to have any unusual features other than that normally associated with the presence of an AF or an AAF adduct (normal sequence) (see Figure 1). The second was the mutational hotspot for AAF mutagenesis in bacteria, the so-called *Nar*I sequence, in which the AF and AAF adducts were positioned on the third guanine from the 5′ end of this sequence (Figure 1). Both substrates were internally labeled with ^{32}P as shown in Figure 1 and contained either an AAF or AF adduct at the indicated positions. These substrates were incubated with the UvrABC nuclease and aliquots were removed over a 30 min time span. The products of these reactions are shown in Figure 2. Several observations can be made concerning this analysis. First, as expected, for each adduct in each sequence a 12 nucleotide product is produced. This was determined by comparison of migration rates of these products with oligonucleotide standards. Second, for the case of the AF adduct located in the *Nar*I sequence, a second product was generated having a chain length of approximately 35 nucleotides (as determined by comparison with standards). This length product indicates that it was formed by the so-called "uncoupled cleavage" that results from incision on the 3′ side of the adduct without concomitant 5′ cleavage. Third, the rate and extent of cleavage, determined by measuring the radioactivity present in each band (Figure 3), indicated that the AAF adduct present in the *Nar*I sequence was cleaved significantly faster and to a greater extent than when this lesion was present in the "normal" non-*Nar*I sequence or when an AF adduct was present in either of these sequences. Interestingly, the sum of all of the 3′ and 5′ cleavage that is detected for the AF adduct present in the *Nar*I sequence (Figures 3 and 4, panels D), equals 70% of the cleavage that occurs for the AAF adduct in the same sequence.

Analysis of the UvrABC Protein−DNA Complexes by SDS Gradient Gel Electrophoresis. It has been suggested that there are several distinct protein−DNA complexes formed during DNA repair mediated by the UvrABC nuclease (Van Houten & Snowden, 1993). In most cases the UvrABC protein−DNA complexes were identified by electrophoresis in buffer systems that are different from the UvrABC nuclease reaction conditions. Therefore, it is possible that a portion of the complexes formed under reaction conditions

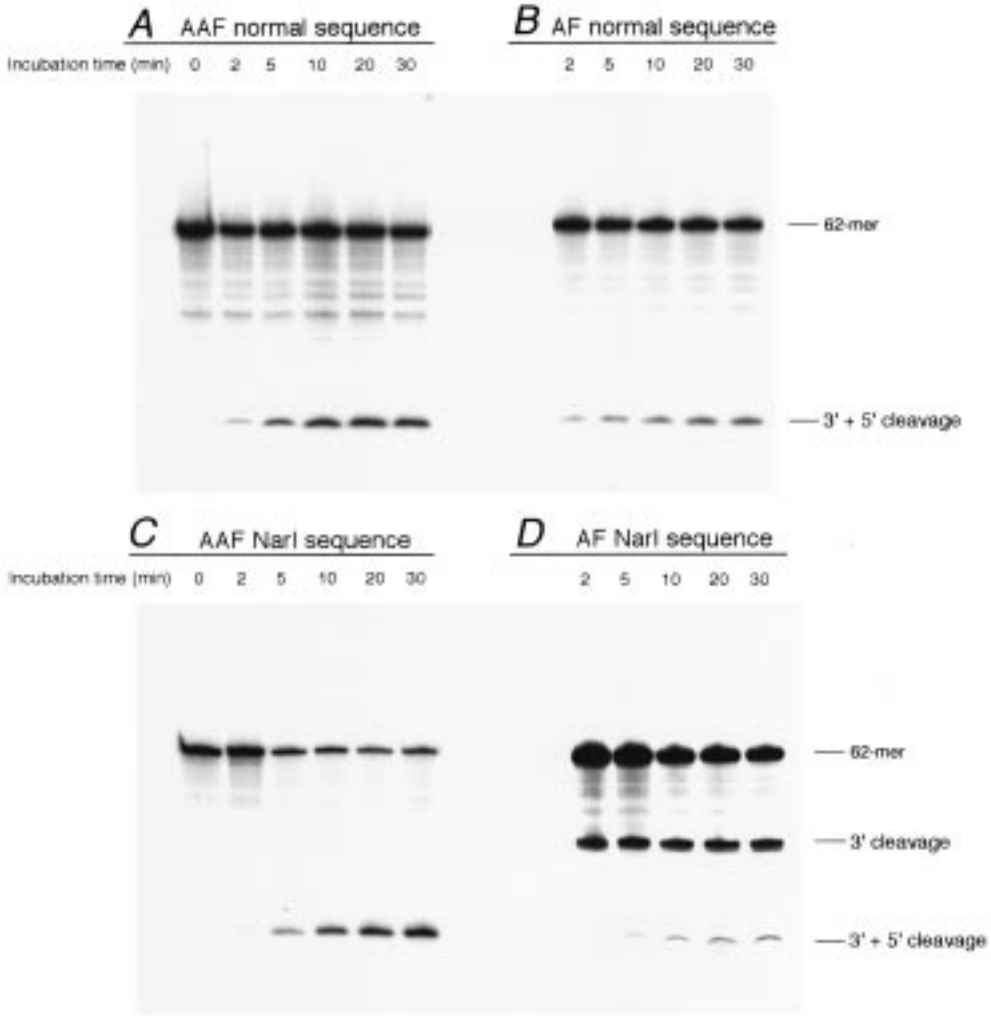

FIGURE 2: UvrABC incision of modified DNA prior to cross-linking. The modified labeled double-stranded 62-mers (0.5 nM) were incubated with 50 nM UvrABC nuclease for the indicated time and the incision products were analyzed on a 15% polyacrylamide denaturing gel as described under Experimental Procedures. Oligonucleotides incised are indicated at the top of each panel.

may dissociate during the analysis. Moreover, these complexes are not stable in denaturing SDS gels that would allow a determination of the molecular weights of the complexes. To stabilize these protein−DNA complexes, we have used a combination of glutaraldehyde and UV light treatment. Glutaraldehyde is a chemical agent that is able to stabilize protein−protein and protein−DNA complexes and acts presumably by fixing the protein conformation through the formation of covalent bonds between the amino acid chains (Lundblad & Noyes, 1984). In these assays, glutaraldehyde was added only after preincubation of the reaction mixtures and therefore it is likely to stabilize the preformed protein−DNA complexes rather than cause their formation. It has also been shown that UV light causes the formation of a covalent linkage between DNA and various DNA-binding proteins in the vicinity of the enzymatically active region of the proteins (Markovitz, 1972; Williams & Konigsberg, 1991). The efficiency of bond formation was shown to be DNA and protein sequence-dependent. Using these methods, the functionally active complexes that formed between the UvrA, UvrB, and UvrC proteins, added individually or in combination, and duplex oligonucleotides containing site-specific AF or AAF adducts remained stable under the conditions used for the SDS−PAGE analysis. Using only UV irradiation to cross-link the DNA-binding reaction mixture of the UvrABC proteins resulted in the formation of one complex with molecular mass 95 kDa (±4 kDa), which closely matched the molecular weight of UvrB protein−DNA complex (UvrB protein, 76.6 kDa; 62-mer, about 19.4 kDa) (data not shown). This is supported by the fact that UvrB protein forms an extremely stable complex with DNA with a half-life of 55 min (Yeung et al., 1986). Pretreatment with glutaraldehyde leads to additional stabilization of protein−DNA complexes (Figure 4), although the stability of the cross-linked species is strongly dependent on the conditions of the cross-linking procedure.

Shown in Figure 4 are the complexes detected by glutaraldehyde and UV cross-linking at 4 °C (Figure 4A) or 37 °C (Figure 4B) formed between the Uvr proteins and the ^{32}P-end labeled normal sequence containing the AF adduct. These are high-resolution denaturing SDS gradient gels in which the identity of the complex was determined from to calculated molecular mass using cross-linked phosphorylase (monomer through hexamer) and cross-linked albumin (monomer through tetramer) as standards. Incubation of the DNA with UvrA protein alone resulted in the formation of two cross-linked species (lane 2) with molecular masses 126 kDa (± 7.5 kDa) and 225 kDa (± 7.5 kDa) (Table 1). These numbers correspond almost exactly to the predicted molecular mass of the UvrA protein−DNA and $UvrA_2$ protein−

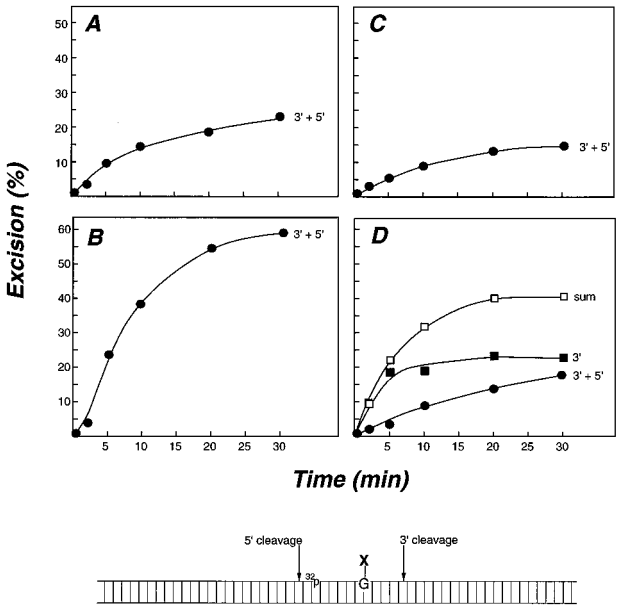

FIGURE 3: Rate of incision of modified 62-mers prior to cross-linking. The extent of the incision for each of the panels shown in Figure 2 was determined by measuring the amount of radioactivity present in each band using a Molecular Dynamics PhosphorImager. The extent of incision is expressed as a percent of the total radioactivity present in each lane and plotted *versus* the incubation time. Data are the mean of two independent experiments. In *panel D* "sum" indicates the sum of the bands produced by 3′ and 3′ + 5′ cleavage. The oligonucleotides used for these reactions were (A) AAF, normal sequence; (B) AAF, *Nar*I sequence; (C) AF, normal sequence; and (D) AF, *Nar*I sequence.

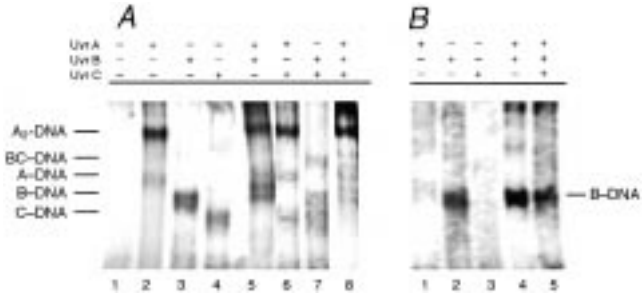

FIGURE 4: SDS−PAGE analysis of the UvrABC protein-DNA complexes cross-linked with glutaraldehyde and UV light. The Uvr proteins (50 nM) were incubated with the AF-modified normal sequence (1 nM) and cross-linked with glutaraldehyde and UV light, and the protein−DNA complexes were separated on a SDS 4−8% gradient polyacrylamide gel as described under Experimental Procedures. Molecular masses were determined by staining a separate portion of the gel using the following protein standards: cross-linked phosphorylase *b*, 97 400 Da, monomer through hexamer, and cross-linked albumin, 66 000 Da, monomer through tetramer. (*A*) Incubation of UvrABC proteins with the oligonucleotide was carried out at 22 °C, chemical cross-linking was conducted on ice, and UV cross-linking was performed at 4 °C. (*B*) Proteins were incubated with the oligonucleotide at 37 °C, cross-linking with glutaraldehyde was conducted on ice, and the reaction mixture was subjected to UV cross-linking at 22 °C.

DNA complexes (Table 1). The presence of both of these complexes indicates that both the UvrA protein monomer and dimer are able to bind DNA, although the weaker band corresponding to the UvrA protein−DNA complex might be an indication of incomplete cross-linking of the UvrA protein subunits. It has been shown that under some conditions, such as high protein concentration, the UvrB protein can bind DNA in the absence of the UvrA protein

Table 1: Molecular Masses of the UvrABC Nuclease−DNA Complexes

complex	predicted molecular mass[a] (kDa)	calculated molecular mass (kDa)
UvrA−DNA	123	125 ± 7
$UvrA_2$−DNA	227	226 ± 7
UvrB−DNA	96	100 ± 5
UvrC−DNA	88	89 ± 5
UvrBC−DNA	164	157 ± 13

[a] Predicted molecular masses were based on the molecular masses of the individual components: UvrA, 103.8 kDa; UvrB, 76.6 kDa; UvrC, 68.1 kDa; single-stranded 62-mer, 19.4 kDa.

(Hsu et al., 1995), and the UvrC alone is able to bind single-stranded DNA with relatively high affinity (Sancar et al., 1981). Our results demonstrate that under conditions used for these experiments both the UvrB and UvrC proteins form complexes with DNA that can be stabilized by cross-linking (Figure 4A, lanes 3 and 4, respectively, and Table 1). Addition of these proteins in different combinations (Figure 4A, lanes 5−8) does not seem to influence the formation of the cross-linked species; the intensity of the observed bands appears to be the same as in the case of the individual proteins added. The only new complex (with molecular mass 157 ± 13.5 kDa) appeared when the B and C subunits were incubated with DNA (Figure 4, lane 7). On the basis of this molecular mass, we assigned this band to the UvrBC protein−DNA complex.

From this analysis it is evident that when the cross-linking is carried out at low temperature, then complexes can be detected between the DNA and each of the individual proteins and to the $UvrA_2$ protein dimer. If the cross-linking is carried out at 37 °C, then only the UvrB protein complex is observed when each of the individual subunits are added. Moreover, the formation of this species is enhanced if the UvrA protein is also present (Figure 4B). It appears that at higher temperature the other complexes are either less stable or these complexes are transient, and once the UvrB protein complex forms, the levels of the other complexes are reduced.

These results demonstrate that combined chemical and UV cross-linking provides a sensitive method to detect and measure the formation of protein−DNA complexes during DNA repair mediated by UvrABC nuclease. Unlike DNA footprinting methods to detect the DNA complexes, this is a direct measure of these species by allowing a direct evaluation of the molecular mass of the cross-linked material. This method is therefore appropriate to measure and compare the rate of complex formation with the rate of incision.

Detection and Characterization of UvrABC Nuclease−DNA Complexes. As mentioned above, combined chemical and UV cross-linking provides a useful tool to characterize protein−DNA complexes formed during the UvrABC nuclease incision repair. To determine the subunit identity and the rate of preincision and incision complex formation for the four adduct and sequence combinations shown in Figure 1, the UvrABC nuclease was incubated with each of these ^{32}P-labeled DNA substrates and then cross-linked with glutaraldehyde and UV light. These complexes were then precipitated with TCA and electrophoresed on an SDS 4−8% gradient gel to determine the molecular masses of the labeled complexes. Shown in Figure 5 is the time course for the

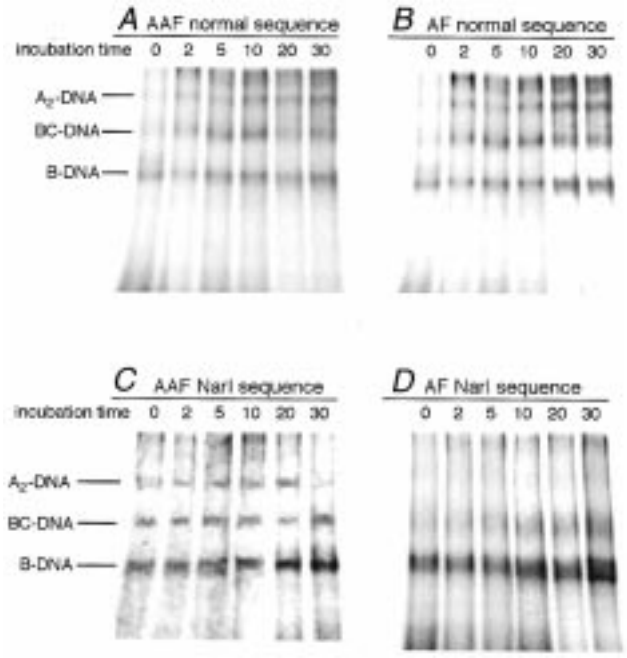

FIGURE 5: Detection of protein−DNA complexes on AAF- and AF-modified oligonucleotides. The AAF- and AF-modified, ^{32}P-labeled duplex 62-mers were incubated with the UvrABC nuclease for the indicated times and then subjected to glutaraldehyde and UV cross-linking as described under Experimental Procedures. The cross-linked complexes were separated on SDS 4−8% gradient PAGE and the autoradiographs of these gels are shown in each panel. Molecular masses were determined by staining a separate portion of the gel using the following protein standards: crosslinked phosphorylase *b*, 97 400 Da, monomer through hexamer, and cross-linked albumin, 66 000 Da, monomer through tetramer). (*A*) AAF, normal sequence; *(B*) AF, normal sequence; (*C*) AAF, *Nar*I sequence; (*D*) AF, *Nar*I sequence.

complex formation that was obtained for each substrate. For each of these gels (repeated in triplicate), three complexes are clearly visible whose molecular masses match the sizes of the predicted complexes, $UvrA_2$−DNA, UvrBC−DNA, and UvrB−DNA (Table 1).

The radioactivity measured in each band was normalized on the basis of the total amount of radioactivity present in each lane and is expressed as a percent of the radioactivity present in the 30-min time point. This procedure is able to compensate for lane to lane differences for the time courses and also for the sequence-derived differences in binding efficiencies. For example, it is known that AT-rich sequences are able to form UV cross-links more efficiently than GC-rich sequences (Williams & Konigsberg, 1991) so that without this normalization method one might obtain differences simply because of the difference in nucleotide composition of the two sequences used. For the experiments described here, the effectiveness of the cross-linking procedure was also found to be sequence-dependent. The *Nar*I sequence, containing G and C bases in the lesion region represents an inefficient substrate for this method, whereas the non-*Nar* I sequence used in this study consists mostly of A and T bases, thus facilitating formation of covalent bonds with the proteins. Therefore it was important to use the normalized data presented in Figure 6.

The results of this analysis are presented in Figure 6. These data shows that the rate at which the UvrB protein−DNA complex forms is nearly identical with the rate at which

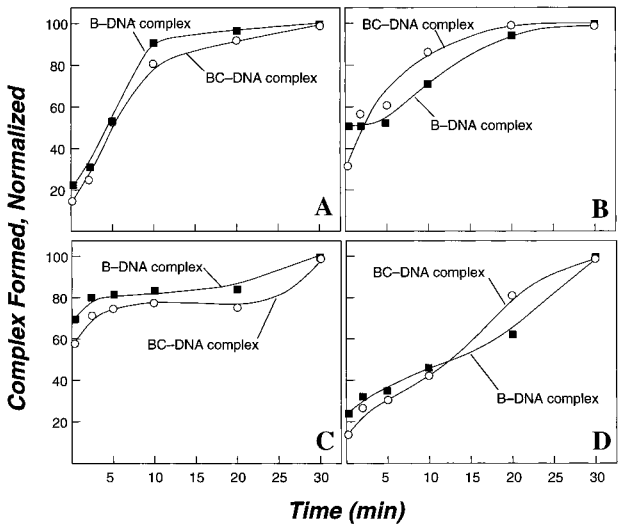

FIGURE 6: Analysis of the UvrB−DNA and UvrBC−DNA complex formation. The level of complex formed in each of the panels shown in Figure 5 was determined by measuring the amount of radioactivity present in each band using a Molecular Dynamics PhosphorImager. The values were normalized on the basis of the total amount of radioactivity present in each lane and are expressed as a percent of the radioactivity present in the 30-min time point. (*A*) AAF, normal sequence; (*B*) AF, normal sequence; (*C*) AAF, *Nar*I sequence; (*D*) AF, *Nar*I sequence.

UvrBC protein−DNA complex forms. Also, the rate of formation of both complexes is most rapid for the AAF *Nar*I sequence, with approximately 60% of the maximal complex formation occurring within the first minute of the incubation. Apparently, in this case the distorted region of DNA is immediately recognized and bound by UvrB and UvrC proteins and the extent of the incision of this lesion is the greatest among the four compared (Figure 3). Interestingly, in the case of the AF *Nar*I sequence (Figure 6D) we see a very different pattern of the complex formation. In this case, there is a slower build-up of the protein complex that is comparable to the rate of incision observed in Figure 3 which may mean that complex formation is rate-limiting in the removal of this adduct in this sequence. The rates of complex formation for the adducts present in the normal sequence shows rates intermediate between those of AF *Nar*I and AAF *Nar*I, again correlating with the $3' + 5'$ incision observed in Figure 3. Finally, it is important to note that it was shown that these complexes are not forming during the extended UV treatment since we found that if glutaraldehyde was added to the proteins prior to addition to the DNA, both incision and binding were inhibited (data not shown).

We have also simultaneously monitored the cleavage that occurs in these cross-linking reactions shown in Figure 5. Following the cross-linking procedure, a portion of the ^{32}P-labeled reaction mixture was electrophoresed on a denaturing polyacrylamide gel, and the result is shown in Figure 7. The radioactivity present in each band on these gels was then analyzed as described for Figure 3 and these data are shown in Figure 8. We find here that the rate and extent of coupled ($3' + 5'$) cleavage obtained in the cross-linked reactions was almost identical to that obtained in the absence of cross-linking (*cf.* Figures 2 and 3 with Figures 7 and 8). As mentioned above, we have found that if glutaraldehyde is added prior to the UvrABC proteins followed by incubation for 30 min at 37° C, that incision is inhibited. Therefore it

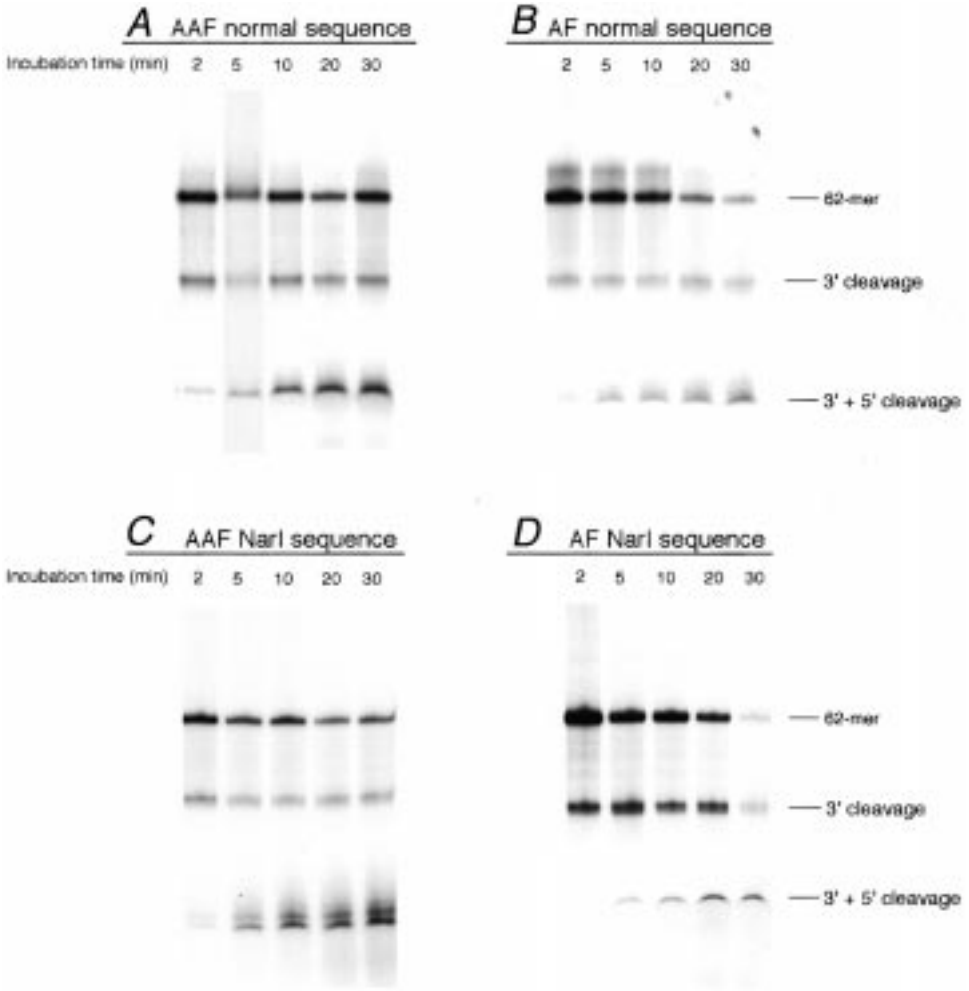

FIGURE 7: UvrABC incision of modified substrate after chemical and UV cross-linking. Duplex ^{32}P-labeled 62-mers (0.5 nM) were incubated with 50 nM UvrABC nuclease for the indicated time and were then subjected to glutaraldehyde and UV cross-linking as described under Experimental Procedures. After precipitation with trichloroacetic acid, the incision products were analyzed on a 15% polyacrylamide denaturing gel. (*A*) AAF, normal sequence; (*B*) AF, normal sequence; (*C*) AAF, *Nar*I sequence; (*D*) AF, *Nar*I sequence.

is not surprising that the incision obtained with or without cross-linking is similar since the majority of the coupled cleavage must have occurred prior the addition of glutaraldehyde and the subsequent UV treatment. However, examination of the gels shown in Figure 7 indicates that, in addition to the product obtained following 3′ + 5′ cleavage, a second band is observed for each sequence that resulted from uncoupled (3′) cleavage. It is interesting that the extent of this cleavage is nearly the same in each case with the exception of the AF adduct in the *Nar*I sequence where this cleavage occurs in the absence of cross-linking. Thus, it is likely that this uncoupled cleavage is occurring subsequent to glutaraldehyde addition and that it results from an enhanced interaction of the Uvr proteins with the DNA induced by the presence of the cross-links.

DISCUSSION

DNA nucleotide excision repair is a complex multistep process that involves an assembly of a DNA−protein complex that must be able to efficiently discriminate between damaged and undamaged sites. It is not completely understood how this specificity is achieved in any system. Because of its relative simplicity, the *E. coli* UvrABC nuclease has served as a model for understanding this damage recognition mechanism. Understanding those structural parameters that direct and modulate UvrABC nuclease action may have wide-ranging biological significance since it seems reasonable that this type of flexibility would be part of repair systems of eukaryotes.

A great deal is known about the mechanism by which the UvrA, UvrB, and UvrC proteins accomplish this damage-specific recognition and excision (Friedberg, 1995; Sancar, 1996). The first step in this process apparently is the ATP-dependent formation of a complex between two UvrA proteins and one UvrB protein to form a $(UvrA)_2UvrB$ protein complex. It is believed that this species then bind to DNA and translocates along the DNA until a damage site is located. The role of this transient protein−DNA complex has been suggested to be to transfer the UvrB subunit to the damage site, producing the highly stable UvrB protein−DNA complex, although the precise role that the $(UvrA)_2UvrB$ protein complex plays in this process is not known in any detail. Some studies have suggested that the rate for UvrB protein loading is slow and may be the rate-limiting step in UvrABC nuclease action. It has also been speculated that the greater the DNA distortion induced by the damage, the greater the stability of the transient $(UvrA)_2UvrB$ protein−DNA complex, which, presumably, might result in a more

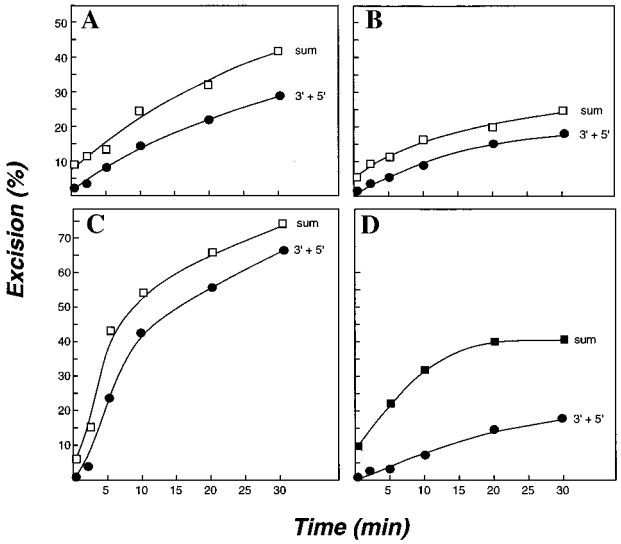

FIGURE 8: Rate of the incision of AAF- and AF-modified oligonucleotides after chemical and UV cross-linking. The extent of the incision for each of the panels shown in Figure 7 was determined by measuring the amount of radioactivity present in each band using a Molecular Dynamics PhosphorImager. The extent incision is expressed as a percent of the total radioactivity present in each lane and plotted *versus* the incubation time. Data are the mean of two independent experiments. In each panel "sum" indicates the sum of the bands produced by 3′ and 3′ + 5′ cleavage. The oligonucleotide used for these reactions were (*A*) AAF, normal sequence; (*B*) AF, normal sequence; (*C*) AAF, *Nar*I sequence; and (*D*) AF, *Nar*I sequence.

rapid loading of the UvrB protein at the damage site (Friedberg, 1995).

Our primary goal in this study was to determine if there were differences in the rates of incision of chemically similar DNA damage by the UvrABC nuclease, to correlate these rates with the rate and extents of protein binding, and to relate these differences to the presumed three-dimensional DNA structures adopted by the adducts. We chose two DNA sequences with site-specific AAF and AF adducts as substrates because the structures of these adducts have been extensively studied. Thus, for these studies we positioned both an AAF and an AF adduct at the G_3 position within a *Nar*I sequence and within a second sequence not expected to have any unusual structural features (see Figure 1). The results obtained clearly indicate that the adduct structure and sequence context do affect the rate and extent of cleavage and that these rates seem to correlate with the expected level of distortion in each situation. Moreover, we have further shown that the rates of cleavage correlate with the rates at which both the UvrB protein−DNA and UvrBC protein−DNA complexes form.

It has been reported previously that the formation the UvrB protein−DNA complex on cisplatin-damaged DNA was fast and did not vary between cisplatin·GG and cisplatin·GCG lesions (Visse et al., 1994). Similarly, studies of four stereoisomers of the benzo[*a*]pyrene diolepoxide lesions revealed no differences in the binding of the $UvrA_2$ or the $UvrA_2B$ protein complex to the DNA (Zou et al., 1995). These results may indicate that the formation of the preincision complexes in these cases is not the rate-limiting step of the endonuclease incision. Contrary to this, Snowden and Van Houten (1991) demonstrated that the formation of the UvrB protein−DNA complex on the AP sites was the rate-limiting factor. Our results demonstrate that the fastest formation of the preincision/incision complexes is with the the AAF *Nar*I structure, which is believed to be the most DNA helix-distortive lesion among the four considered cases. Interestingly, the *Nar*I site modified with the AF adduct exhibited a different complex formation pattern compared with all of the other substrates we used. Both the UvrB−DNA and UvrBC−DNA complexes formed significantly more slowly, demonstrating that this could be a rate-limiting step. Moreover, in this case we observe a large fraction of uncoupled (3′) cleavage (Figure 2) that was not seen in the other cases. It is interesting to speculate that these observations are related mechanistically. Nonetheless, the results presented here confirm the hypothesis that distortion imposed on the DNA helix by the AF adduct in the *Nar*I site differs from that induced by the AAF adduct. The lower degree of incision of the AF and AAF adduct in the normal sequence and the correspondingly slower formation of the protein−DNA complexes in these cases imply that the extent of distortion of the adducts in DNA might alter the rate at which the preincision complex forms and thereby slow the rate of cleavage.

The mechanism of damage recognition by the UvrABC nuclease has been the subject of intense interest and speculation. Early models suggested that a backbone deformity in the DNA helix is the main determinant of recognition and ultimate complex formation by the UvrB protein (Sancar & Sancar, 1988; Grossman & Thiagalingam, 1993). More recently, it has been shown that the UvrB protein damage complex is not sensitive to ionic strength (Orren et al., 1992; Orren & Sancar, 1989), implying that the damage may reside in a hydrophobic pocket within the UvrB protein that has the ability to accommodate a wide variety of structures (Hsu et al., 1995). It has also been speculated that ultimate recognition may result in a conformational change in the DNA at the adduct site, which would imply that the strength of binding might involve an interplay between the initial substrate structure and the ultimate structure induced following binding (Friedberg et al., 1995). However, since the rates of cleavage and rates of binding both correlate with the anticipated distortion present in the duplex DNA prior to binding, then some aspect of the initial substrate structure is likely to be present in this final complex. Future studies to better characterize this preincision complex and the use of other adduct structures may provide important clues to understanding how the UvrABC nuclease recognizes and repairs the broad range of DNA lesions.

ACKNOWLEDGMENT

We are grateful to Dr. Yongqi Yong for his aid in the implementation of the cross-linking technique used in this study, to Miss Annie Pao and Mr. Yi Zheng for purifying the UvrABC nuclease, and to Dr. Ashok Bhagwat for critically reading the manuscript.

REFERENCES

Alazard, R., Germanier, M., & Johnson, N. P. (1982) *Mutat. Res. 93*, 327−337.

Belguise-Valladier, P., & Fuchs, R. P. P. (1991) *Biochemistry 30*, 10091−10100.

Belguise-Valladier, P., & Fuchs, R. P. P. (1995) *J. Mol. Biol. 249*, 903−913.

Bichara, M., & Fuchs, R. P. P. (1985) *J. Mol. Biol. 183*, 341−351.
Burnouf, D., Koehl, P., & Fuchs, R. P. P. (1989) *Proc. Natl. Acad. Sci. U.S.A. 86*, 4147−4151.
Cho, B. P., Beland, F. A., & Marques, M. M. (1994) *Biochemistry 33*, 1373−1384.
Eckel, L. M., & Krugh, T. P. R.. (1994) *Biochemistry 33*, 13611−13624.
Friedberg, E. C., Walker, G. C., & Siede, W. (1995) in *DNA Repair and Mutagenesis*, ASM Press, Washington, DC.
Grossman, L., & Thiagalingam, S. (1993) *J. Biol. Chem. 268*, 16871−16874.
Hingerty, B. E., & Broyde, S. (1986) *J. Biomol. Struct. Dyn. 4*, 365−372.
Hsu, D. S., Kim, S.-T., Sun, Q., & Sancar, A. (1995) *J. Biol. Chem. 270*, 8319−8327.
Jones, B., & Yeung, A. T. (1988) *Proc. Natl. Acad. Sci. U.S.A. 85*, 8410−8414.
King, C. M. (1985) in *Prostaglandins, Leukotrienes, and Cancer* (Marnett, L. J., Ed.) Vol. 2, Martinus-Nijhoff, New York.
Koehl, P., Valladier, P., Lefevre, J.-F., & Fuchs, R. P. P. (1989) *Nucleic Acids Res. 17*, 9531−9541.
Koffel-Schwartz, N., Verdier, J.-M., Bichara, M., Freund, A.-M., Daune, M. P., & Fuchs, R. P. P. (1984) *J. Mol. Biol. 177*, 33−51.
Lambert, B., Jones, B. K., Roques, B. P., Le Pecq, J.-B., & Yeung, A. T. (1989) *Proc. Natl. Acad. Sci. U.S.A. 86*, 6557−6561.
Lin, J.-J., & Sancar, A. (1992) *Mol. Microbiol. 6*, 2219−2222.
Lin, J.-J., Philips, A. M., Hearst, J. E., & Sancar, A. (1992) *J. Biol. Chem. 267*, 17693−17700.
Lundblad, R. L., & Noyes, C. M. (1984) in *Chemical Reagents for Protein Modification*, Vol. II, CRC Press, Boca Raton, FL.
Markovitz, A. (1972) *Biochim. Biophys. Acta 281*, 522−534.
Moolenaar, G. F., Franken, K. L., Dijkstra, D. M., Thomas-Oates, J. E., Visse, R., van de Putte, P., & Goosen, N. (1995) *J. Biol. Chem. 270*, 30508−30515.
Norman, D., Abuaf, P., Hingerty, B. E., Live, D., Grunberger, D., Broyde, S., & Patel, D. (1989) *Biochemistry 28*, 7462−7476.
O'Handley, S. F., Sanford, D. G., Xu, R., Lester, C. C., Hingerty, B. E., Broyde, S., & Krugh, T. P. R.. (1993) *Biochemistry 32*, 2481−2497.
Orren, D. K., & Sancar, A. (1989) *Proc. Natl. Acad. Sci. U.S.A. 86*, 5237−5241.
Orren, D. K., Selby, C. P., Hearst, J. E., & Sancar, A. (1992) *J. Biol. Chem. 267*, 780−788.
Pierce, J. R., Case, R., & Tang, M. S. (1989) *Biochemistry 28*, 5821−5826.
Ramaswamy, M., & Yeung, A. T. (1994) *J. Biol. Chem. 269*, 485−492.
Sancar, A. (1996) *Annu. Rev. Biochem. 65*, 43−81.
Sancar, A., & Rupp, W. D. (1983) *Cell 33*, 249−260.
Sancar, A., & Tang, M.-S. (1993) *Photochem. Photobiol. 57*, 905−927.
Sancar, A., Franklin, K. A., Sancar, G., & Tang, M. S. (1985) *J. Mol. Biol. 184*, 725−734.
Seeberg, E., & Fuchs, R. (1990) *Proc. Natl. Acad. Sci. U.S.A. 87*, 191−194.
Selby, C., & Sancar, A. (1991) *Biochemistry 30*, 3841−3849.
Shibutani, S., Gentles, R., Johnson, J., & Grollman, A. P. (1991) *Carcinogenesis 12*, 813−818.
Singer, B., & Grunberger, D. (1984) *Molecular Biology of Mutagens and Carcinogens*, Plenum Press, New York.
Snowden, A., & Van Houten, B. (1991) *J. Biol. Chem. 220*, 19−33.
Tang, M. S. (1996) in *Technologies for Detection of DNA Damage and Mutations* (Pfeifer, G. P., Ed.) pp 139−153, Plenum Press, New York.
Tang, M., Lieberman, M. W., & King, C. M. (1982) *Nature 299*, 646−648.
Tebbs, R. S., & Romano, L. J. (1994) *Biochemistry 33*, 8998−9006.
van Houte, L. P. A., Bokma, J. T., Lutgerink, J. T., Westra, J. G., Retel, J., & van Grondelle, R. (1987) *Carcinogenesis 8*, 759−766.
van Houte, L. P. A., Westra, J. G., Retel, J., van Grondelle, R., & Blok, J. (1988) *Carcinogenesis 9*, 1017−1027.
Van Houten, B., & Snowden, A. (1993) *BioEssays 15*, 51−59.
Visse, R., van Gool, A. J., Moolenaar, G. F., de Ruijter, M., & van de Putte, P. (1994) *Biochemistry 33*, 1804−1811.
Weber, K., & Osborn, M. (1969) *J. Biol. Chem. 244*, 4406.
Williams, K. R., & Konigsberg, W. H (1991) *Methods Enzymol. 208*, 516−539.
Zhou, Y., & Romano, L. J. (1993) *Biochemistry 32*, 14043−14052.
Zou, Y., Liu, T.-M., Geacintov, N. E., & Van Houten, B. (1995) *Biochemistry 34*, 13582−13593.

BI971544P